

Supporting Information

Highly Polar Stacking Where Organics Wraps Inorganics: Lone-pair- π -Hole Interactions between the PdO₄ Core and Electron-deficient Arenes

Yury V. Torubaev ^a, Ivan V. Skabitsky ^a, Anton Rozhkov ^b, Bartomeu Galmés ^c, Antonio Frontera ^c, Vadim Yu. Kukushkin ^{b,d}

^a*N. S. Kurnakov Institute of General and Inorganic Chemistry, of Russian Academy of Sciences, Moscow, 119991 Russian Federation*

^b*Institute of Chemistry, Saint Petersburg State University, Universitetskaya Nab. 7/9, Saint Petersburg, 199034 Russian Federation*

^c*Departament de Química, Universitat de les Illes Balears, Crta de Valldemossa km 7.5, 07122 Palma de Mallorca (Balears), Spain*

^d*Institute of Chemistry and Pharmaceutical Technologies, Altai State University, 656049 Barnaul, Russian Federation*

Section S1: Experimental data, structural information and Hirshfeld analysis

Table S1. X-Ray Crystal data and structure refinement for [Pd₃]·(FN), [Pd₃]·(4,4'-FBph), [Pd₃]·(IFB), [Pd₃]·(IFTol), [Pd₃]·(1,4-IFB) and [Pd₃]·(1,2-IFB)

	[Pd ₃]·(FN)	[Pd ₃]·(4,4'-FBph)	[Pd ₃]·(IFB)	[Pd ₃]·(IFTol)	[Pd ₃]·(1,4-IFB)	[Pd ₃]·(1,2-IFB)
CCDC	2082585	2082584	2082583	2082586	2082588	2082587
Empirical formula	C ₃₂ H ₁₈ F ₁₆ O ₁₂ Pd ₃	C ₄₉ H ₃₈ Cl ₂ F ₁₆ I ₄ O ₂₄ Pd ₆	C ₁₈ H ₁₈ F ₅ IO ₁₂ Pd ₃	C ₁₉ H ₁₈ F ₇ IO ₁₂ Pd ₃	C ₁₈ H ₁₈ F ₄ I ₂ O ₁₂ Pd ₃	C ₂₄ H ₁₈ F ₈ I ₄ O ₁₂ Pd ₃
Formula weight	1217.66	2531.69	967.42	1017.43	1075.32	1477.18
Temperature/K	100.0	150.0	100.0	150.0	100.0	103.0
Crystal system	monoclinic	monoclinic	monoclinic	orthorhombic	monoclinic	triclinic
Space group	P2 ₁ /m	C2/c	P2 ₁ /n	Imma	P2 ₁ /n	P-1
a/Å	8.3099(3)	54.001(2)	8.4389(5)	15.4555(5)	18.4749(7)	8.4878(3)
b/Å	16.8417(5)	8.2670(4)	19.8050(11)	18.5032(6)	18.3530(7)	10.1254(4)
c/Å	14.1454(4)	15.6172(8)	16.1256(9)	10.1571(3)	18.4759(7)	22.1613(8)
α/°	90	90	90	90	90	84.6430(10)
β/°	105.7220(10)	97.470(2)	96.095(2)	90	113.0370(10)	85.0080(10)
γ/°	90	90	90	90	90	77.8580(10)
Volume/Å ³	1905.62(10)	6912.7(6)	2679.9(3)	2904.69(16)	5765.0(4)	1849.41(12)
Z	2	4	4	4	8	2
ρ _{calc} /cm ³	2.122	2.433	2.398	2.327	2.478	2.653
μ/mm ⁻¹	1.540	3.508	3.235	3.001	4.073	4.876
F(000)	1176.0	4760.0	1832.0	1928.0	4016.0	1360.0
Crystal size/mm ³	0.18 × 0.14 × 0.1	0.11 × 0.09 × 0.06	0.23 × 0.14 × 0.02	0.13 × 0.09 × 0.07	0.15 × 0.11 × 0.08	0.27 × 0.18 × 0.16
Radiation	MoKα (λ = 0.71073)					
2θ range for data collection/°	3.846 to 65.214	4.564 to 58.318	4.114 to 55.806	4.402 to 65.18	2.642 to 65.286	4.126 to 59.992
Index ranges	-12 ≤ h ≤ 12, -25 ≤ k ≤ 25, -21 ≤ l ≤ 21	-74 ≤ h ≤ 73, 0 ≤ k ≤ 11, 0 ≤ l ≤ 21	-11 ≤ h ≤ 11, 0 ≤ k ≤ 26, 0 ≤ l ≤ 21	-23 ≤ h ≤ 23, -28 ≤ k ≤ 28, -15 ≤ l ≤ 15	-28 ≤ h ≤ 28, -27 ≤ k ≤ 27, -28 ≤ l ≤ 28	-11 ≤ h ≤ 11, -14 ≤ k ≤ 14, -31 ≤ l ≤ 31
Reflections collected	103202	12125	11763	54105	454623	176027
Independent reflections	7171 [R _{int} = 0.0294, R _{sigma} = 0.0125]	12125 [R _{int} = 0.2375, R _{sigma} = 0.0307]	11763 [R _{int} = 0.1215, R _{sigma} = 0.0301]	54105 [R _{int} = 0.2039, R _{sigma} = 0.0504]	21079 [R _{int} = 0.0403, R _{sigma} = 0.0200]	10751 [R _{int} = 0.0392, R _{sigma} = 0.0139]
Data/restraints/parameters	7171/54/408	12125/0/463	11763/0/357	54105/9/162	21079/28/848	10751/90/570
Goodness-of-fit on F ²	1.123	1.112	1.160	1.110	1.082	1.142

Final R indexes [$I \geq 2\sigma(I)$]	$R_1 = 0.0299,$ $wR_2 = 0.0709$	$R_1 = 0.0320,$ $wR_2 = 0.0739$	$R_1 = 0.0624,$ $wR_2 = 0.1415$	$R_1 = 0.0450,$ $wR_2 = 0.0917$	$R_1 = 0.0340,$ $wR_2 = 0.0685$	$R_1 = 0.0250,$ $wR_2 = 0.0582$
Final R indexes [all data]	$R_1 = 0.0329, wR_2 =$ 0.0726	$R_1 = 0.0402,$ $wR_2 = 0.0759$	$R_1 = 0.0761, wR_2 =$ 0.1492	$R_1 = 0.0602, wR_2 =$ 0.0979	$R_1 = 0.0489, wR_2 =$ 0.0771	$R_1 = 0.0269, wR_2 =$ 0.0590
Largest diff. peak/hole / $e \text{ \AA}^{-3}$	1.44/-1.46	0.75/-0.77	2.37/-1.89	0.98/-0.92	1.96/-2.61	1.56/-1.58

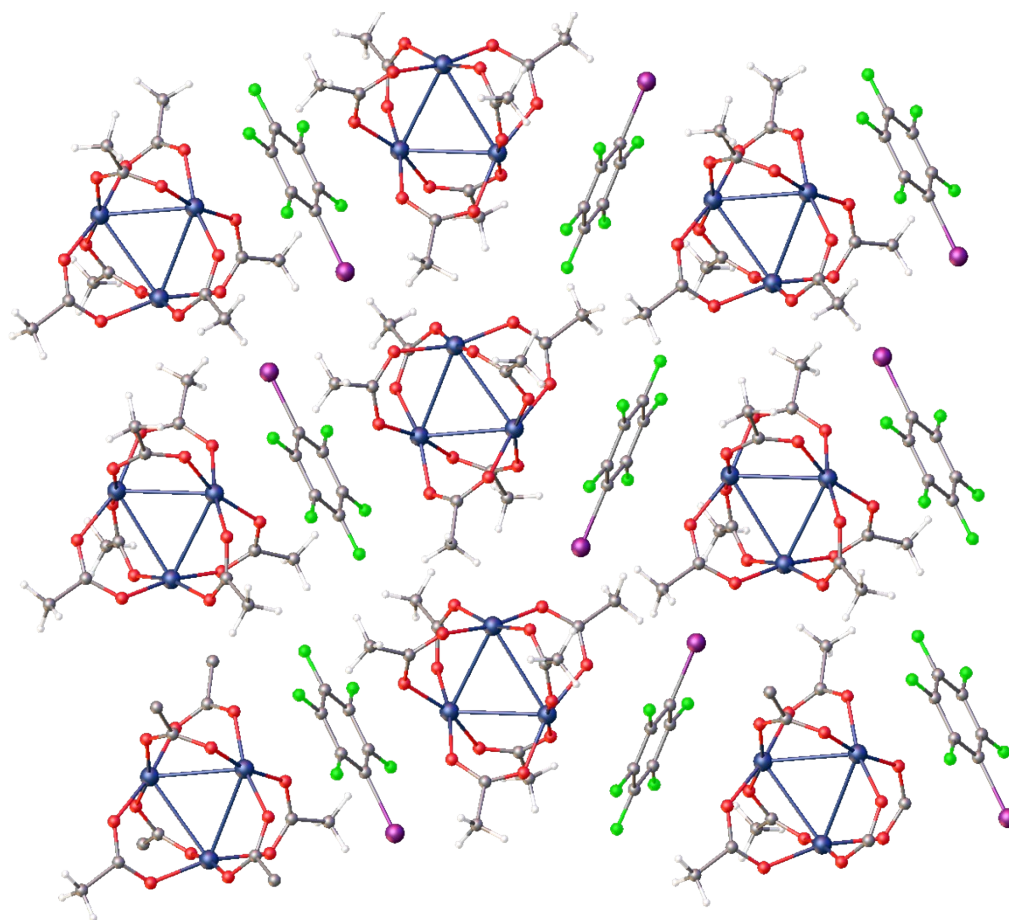


Figure S1. Crystal structure diagram of $[\text{Pd}_3] \cdot (\text{IFB})$; $\text{I} \cdots \text{O}$ 2.951(8), $\text{Pd1} \cdots \text{IFB}$ centroid 3.481–3.532 Å; $\angle(\text{C}-\text{I} \cdots \text{O})$ 170.2(4); torsion angle $\angle(\text{Me}-\text{C}-\text{O} \cdots \text{I})$ 53(1)°. The angle between the PdO_4 and C_6 planes is 2.5°.

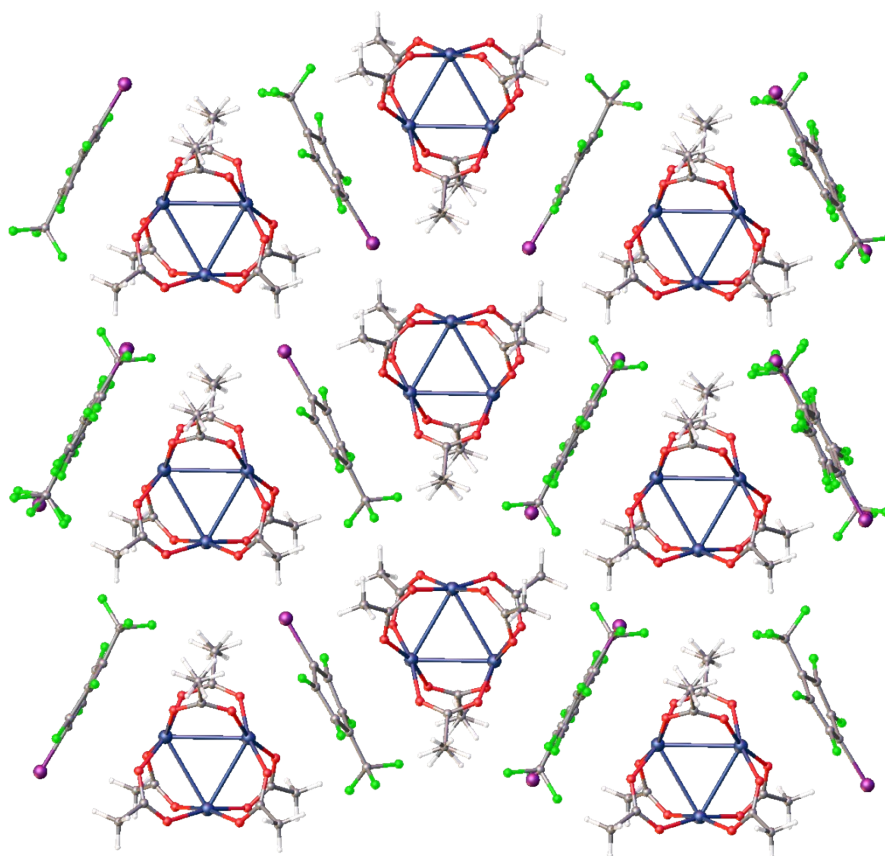


Figure S2. Crystal structure diagram of $[\text{Pd}_3]\cdot(\text{IFTol})$; $\text{I}\cdots\text{O}$ 3.348(5)–3.517(5) Å. Positions of I and CF_3 functions in IFTol molecules are disordered with 50% occupancy but some of them are not shown as disordered for clarity. The unit cell parameters for $[\text{Pd}_3]\cdot(1,4\text{-IFB})$ (*Imma*; a 15.4548(5), b 18.5028(6), c 10.1568(3) Å) and $[\text{Pd}_3]\cdot(\text{IFTol})$ (*Imma*; a 15.4187(6), b 17.9469(7), c 10.2344(4) Å) are quite similar.

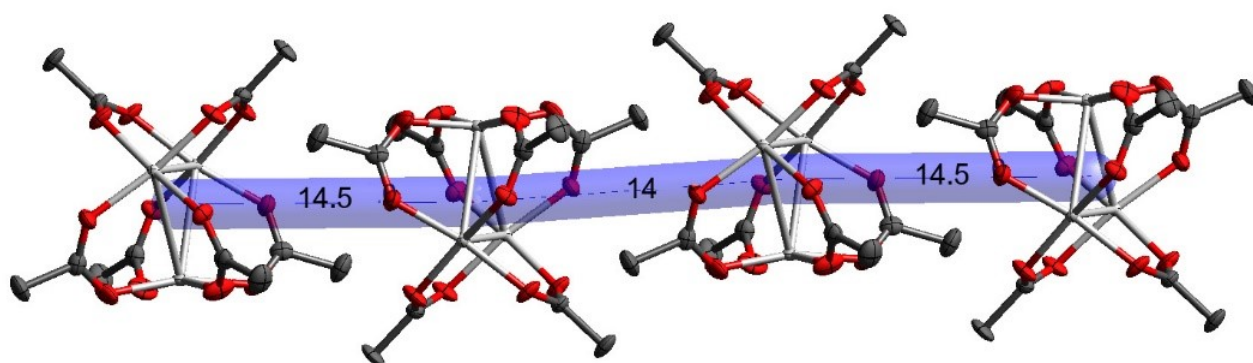


Figure S3. The energy framework of $[\text{Pd}_3]\cdot(1,4\text{-IFB})$ showing the chain of $[\text{Pd}_3]$. Intermolecular energies are shown in kcal/mol.

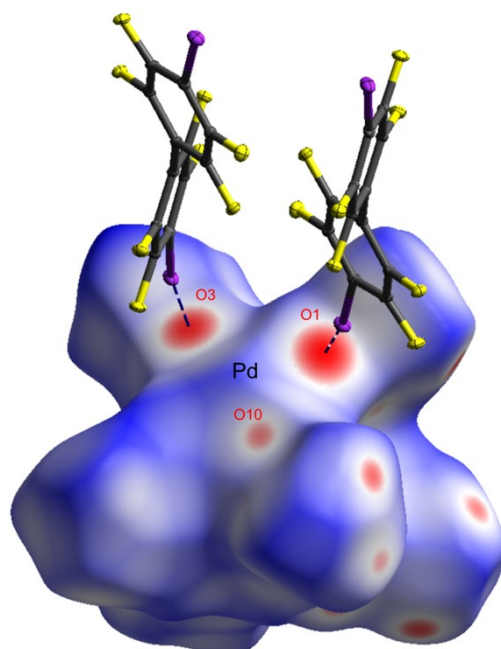


Figure S4. Hirshfeld surface map (d_{norm}) for $[\text{Pd}_3] \cdot (4,4'\text{-IFBph})$; the red areas indicate unbifurcated two-center $\text{I} \cdots \text{O}$ HaBs, while blue areas reflect the absence of short noncovalent contacts.

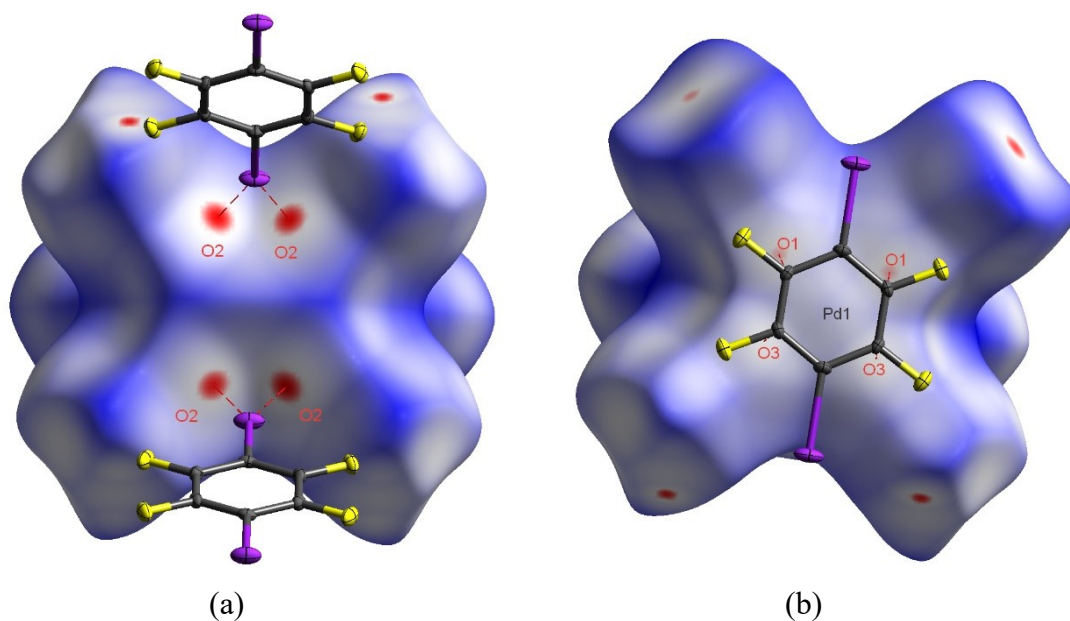


Figure S5. Hirshfeld surface map (d_{norm}) for $[\text{Pd}_3] \cdot (1,4\text{-IFB})$; (a) red areas are due to $\text{I} \cdots \text{O}$ HaBs (b) while white areas correspond to short $\text{Pd} \cdots \text{C}$ and $\text{O} \cdots \text{C}$ contacts.

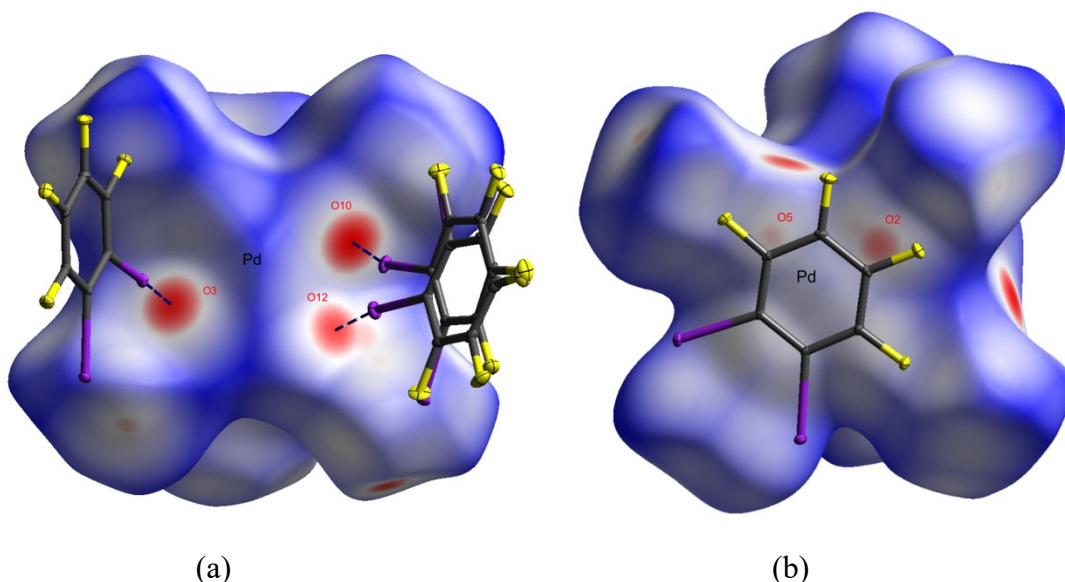


Figure S6. Hirshfeld surface map (d_{norm}) for $[\text{Pd}_3]\cdot(1,2\text{-IFB})$; (a) red areas are due to short two-centered, not bifurcated $\text{I}\cdots\text{O}$ HaBs (disorder of iodine atoms in 1,2-IFB results in two close contacts: $\text{I}3\cdots\text{O}10$ and $\text{I}4\text{A}\cdots\text{O}12$) (b) white areas correspond to $\text{Pd}\cdots\text{C}$ and $\text{O}\cdots\text{C}$ contacts. Blue areas reflect the absence of short noncovalent contacts.

Section S2: Cooperativity and NBO results.

S2.1 cooperativity

Since the $[\text{Pd}_3]$ cluster is acting as the electron donor for both the σ -hole and π -hole interactions, it is expected that, in the multicomponent assemblies, unfavorable cooperativity effects occur. That is, the participation of the cluster in one interaction (either σ -hole or π -hole) with the electron acceptor (arene) reduces the nucleophilicity of the cluster, diminishing its ability to participate in a second interaction (either σ -hole or π -hole). To illustrate this issue, we have used two dimers of $[\text{Pd}_3]\cdot(\text{IFB})$, which are represented in Fig. S7. The MEP surface plot of the HaB dimer (Fig. S7a) shows that the MEP value over the Pd atom is -10.2 kcal/mol, which is less negative than the MEP at the Pd atom in the cluster (i.e. -16.4 kcal/mol, see Fig. 3b in the main text). Similarly, the MEP surface plot of the π -hole dimer (Fig. S7b) shows that the MEP value at the iodine's σ -hole is reduced from 39.6 kcal/mol (see Table 1, main text) to 28.8 kcal/mol. Moreover, the MEP value over a second Pd atom is -9.4 kcal/mol, which is less negative than the MEP at the Pd atom in the cluster. Therefore, from an electrostatic point of view, it is anticipated that the existence of anti-cooperativity effects between σ -hole and π -hole interactions. Other contributions different from electrostatic, may compensate to some extent the unfavorable interplay between both interactions, like polarization and dispersion forces, which are expected to increase in the multicomponent assemblies with respect to the isolated dimers. In fact, we have calculated the cooperativity effects using the methodology proposed in the literature (see equation in Scheme 1)^{S1} for the trimers $(\text{IFTol})\cdot[\text{Pd}_3]\cdot(\text{IFTol})$, $(1,2\text{-IFB})\cdot[\text{Pd}_3]\cdot(1,2\text{-IFB})$, $(1,4\text{-IFB})\cdot[\text{Pd}_3]\cdot(1,4\text{-IFB})$ and $(\text{IFB})\cdot[\text{Pd}_3]\cdot(\text{IFB})$. The values are gathered in Table S2, showing very small and positive E_{coop} values, thus evidencing that the expected anti-cooperativity effects are almost negligible in these systems.

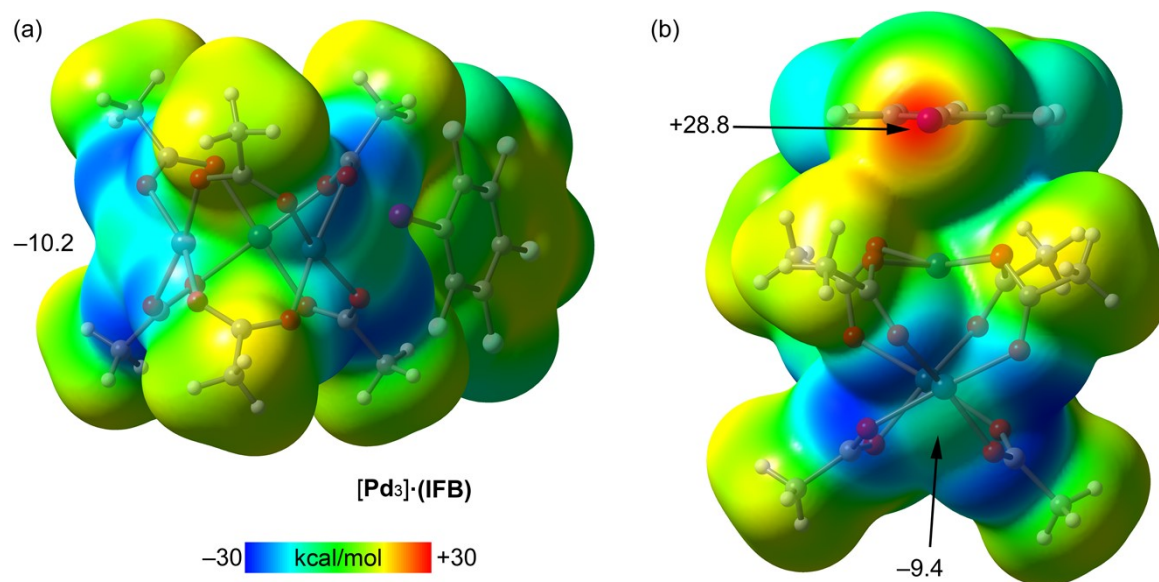
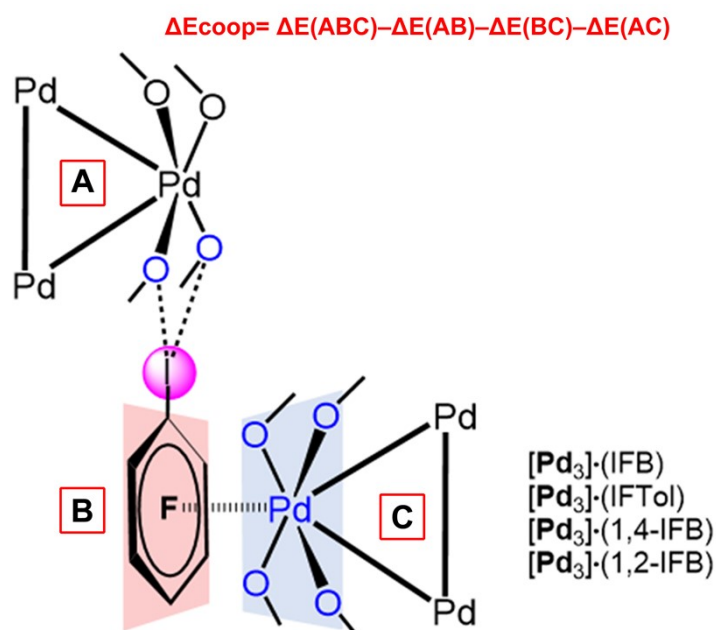


Fig. S7. MEP plots for O...I σ -hole (a) and LP... π -hole dimers of [Pd₃]·(IFB) (b) using the 0.001 au electron density isosurface. Energies in kcal/mol.

Table S2. Cooperativity energies for the trimers represented in Scheme S1 in kcal/mol

Trimer	ΔE_{coop}
(IFTol)·[Pd ₃]·(IFTol)	0.23
(1,2-IFB)·[Pd ₃]·(1,2-IFB)	0.13
(1,4-IFB)·[Pd ₃]·(1,4-IFB)	0.06
(IFB)·[Pd ₃]·(IFB)	0.10



Scheme S1. Trimers used to evaluate cooperativity effects

S2.2 NBO calculations

In order to investigate the lone-pair- π -Hole Interactions between the Pd-atom and the electron-deficient arene, from an orbital point of view, we have performed the natural bond orbital analysis since it is convenient to analyze orbital donor-acceptor interactions based on the second order perturbation analysis.^{S2} We have examined the π -hole interaction in the exemplifying [Pd₃]·(IFB) complex and found several donor-acceptor interactions between the PdO₄ core and the arene. Interestingly, one important donor-acceptor interaction involves the d_{z^2} [Pd] orbital as donor and an antibonding $\pi^*(\text{C}=\text{C})$ orbital of the aromatic ring as acceptor with a concomitant stabilization energy of $E^{(2)} = 2.22$ kcal/mol, thus confirming that the d_{z^2} orbital is the one acting as LP. Fig. S8 shows the representation of the NBOs involved in this particular donor-acceptor interaction. The NBO analysis also reveals a small electron donation from the LP(O) orbitals to antibonding $\pi^*(\text{C}=\text{C})$ orbitals, with a total $E^{(2)} = 0.43$ kcal/mol. This small LP(O) \rightarrow $\pi^*(\text{C}=\text{C})$ contribution is likely due to the separation of the arene with respect to the PdO₄ plane allowing a negligible orbital overlap of the π -orbitals with the oxygen lone pairs. The total orbital contribution is small (2.65 kcal/mol) compared with the total interaction energy of this dimer (-12.6 kcal/mol, see Fig. 11a, main text), thus suggesting that other contributions like electrostatic/polarization/dispersion forces are more dominant.

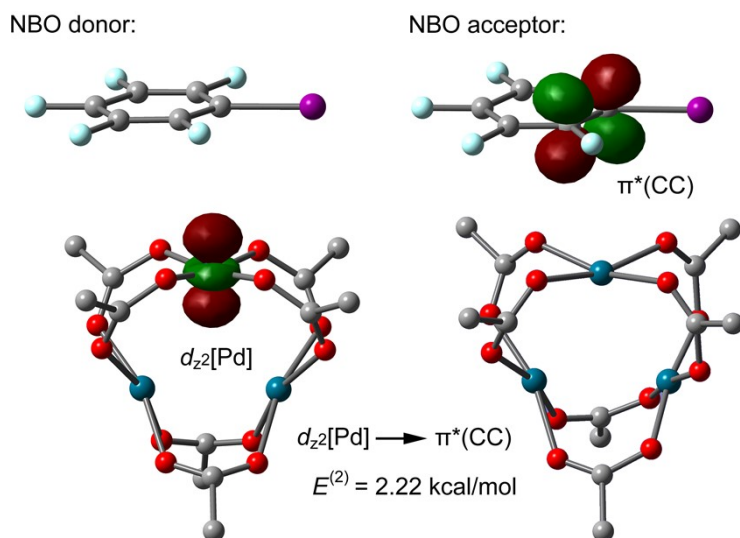


Fig. S8. NBOs involved in the donor-acceptor interaction at the PB97D3/def2-TZVP level of theory

References:

- S1 I. Alkorta, F. Blanco, P. M. Deya, J. Elguero, C. Estarellas, A. Frontera and D. Quiñonero, *Theor. Chem. Acc.*, 2010, **126**, 1-14
- S2 F. Weinhold, C. R. Landis and E. D. Glendening, *Int. Rev. Phys. Chem.*, 2016, **35**, 399-440.